

Reactions of dichloro-substituted iron(II) clathrochelate with 1,4-dioxane radical derivatives: synthesis, structure, and spectral characteristics of the dioxane ring opening product in the ribbed fragment of the macrobicyclic ligand*

M. A. Vershinin,^a A. B. Burdukov,^{a*} Z. A. Starikova,^b V. V. Novikov,^b and Ya. Z. Voloshin^{b*}

^aA. V. Nikolaev Institute of Inorganic Chemistry, Siberian Branch of the Russian Academy of Sciences, 3 prosp. Lavrent'eva, 630090 Novosibirsk, Russian Federation.

Fax: +7 (383) 330 9489. E-mail: lsc@niic.nsc.ru

^bA. N. Nesmeyanov Institute of Organoelement Compounds, Russian Academy of Sciences, 28 ul. Vavilova, 119991 Moscow, Russian Federation.

Fax: +7 (499) 135 5085. E-mail: voloshin@ineos.ac.ru

A free-radical substitution for the chlorine atoms with the 1,4-dioxan-2-yl fragment in the tris-dichloro-substituted dioximate iron(II) clathrochelate is accompanied by the oxidative dioxane ring opening as a side process. The compound obtained was characterized by elemental analysis data, 1D and 2D ¹H and ¹³C{¹H} NMR spectroscopy (in solution), MALDI TOF mass spectrometry, as well as by single-crystal X-ray diffraction.

Key words: clathrochelates, reactions of coordinated ligands, free-radical reactions.

Reactive transition metal macrobicyclic tris-dioximates are promising molecular platforms for the design of multi-functional and polytopic systems with preselected physical and physicochemical properties.¹ To date, in most cases the ribbed functionalization of clathrochelates was being accomplished by nucleophilic substitution for the reactive halogen atoms in their chelate α -dioximate fragments with different N,O,S,C-nucleophiles,^{2–11} as well as by the *in situ* generation of nucleophilic clathrochelate anions *via* deprotonation of substituents in their ribbed fragments.¹⁰

Recently, we have reported a new approach to the functionalization of tris-dioximate iron(II) clathrochelates *via* a free-radical substitution for the ribbed chlorine atoms in the clathrochelate precursors FeBd₂(Cl₂Gm)(BF)₂ (where Bd^{2–} and Cl₂Gm^{2–} are the α -benzyldioximate and dichloroglyoximate dianions, respectively, Scheme 1, complex **1**) with the carbon-centered free radicals, primarily with the 1,4-dioxane radical derivatives.¹² In the present work, we report synthesis, structural and spectral characteristics of a clathrochelate with the ribbed substituent resulted from the 1,4-dioxane ring opening.

Results and Discussion

Heating 1,4-dioxane in the presence of peroxides, including autogenic ones,¹³ leads to the formation of the

carbon-centered 1,4-dioxan-2-yl free radicals.^{14,15} As it has been shown earlier,¹² these radicals can substitute for the reactive chlorine atoms in the dichloro-substituted clathrochelate precursor **1** (see Scheme 1) giving the monoribbed-functionalized mono- and disubstituted macrobicyclic complexes **2** and **3**.

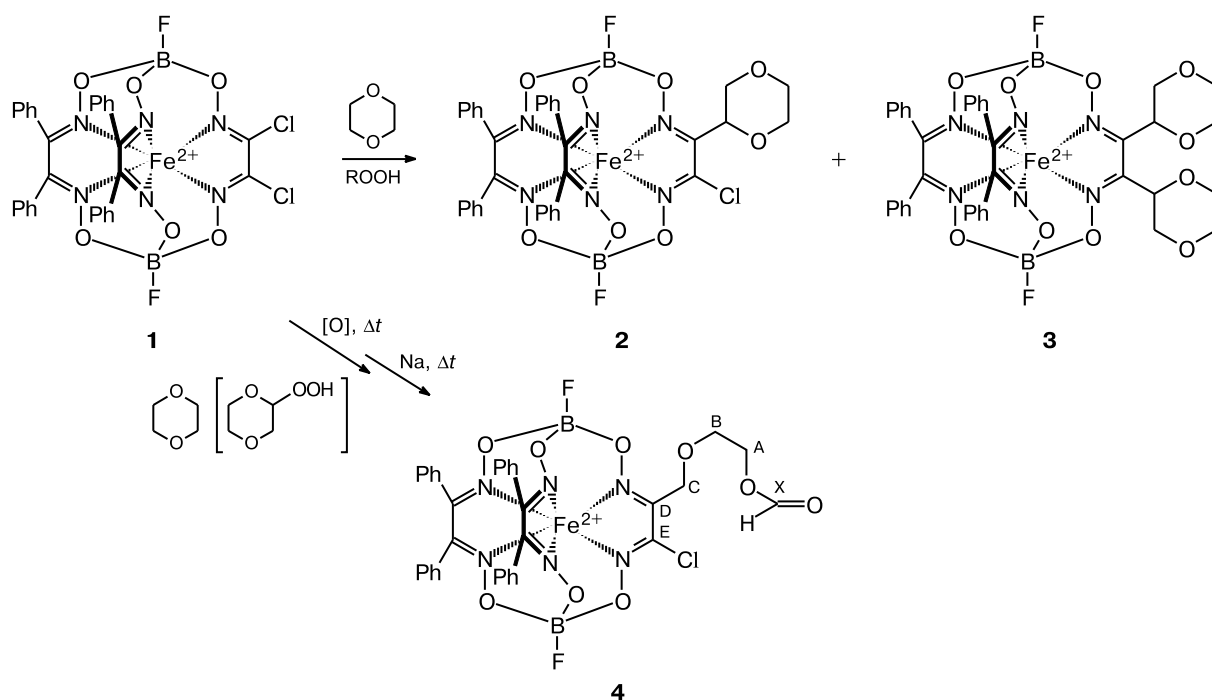
In the present studies, we found that successive reflux of the macrobicyclic precursor **1** first in crude 1,4-dioxane contaminated with its hydroperoxide and then in the presence of metallic sodium led to complex **4** containing no 1,4-dioxan-2-yl fragment (see Scheme 1).

The compound obtained was characterized by elemental analysis, EAS and MALDI-TOF spectra; its composition and structure were established in the solution using one- and two-dimensional ¹H, ¹³C, and ¹⁹F NMR spectra and in the crystal by X-ray diffraction analysis.

Figures 1–3 show the ¹H, ¹³C, and ¹⁹F NMR spectra of complex **4** solution in CD₂Cl₂. As it is seen from Figure 1, in addition to the poorly resolved set of signals for the protons of the ribbed phenyl substituents, the ¹H NMR spectrum contains a downfield singlet signal at δ_H 7.94, as well as upfield signals, whose splitting and integral intensities allowed us to assign them to the protons of the two spin coupled methylene groups (δ_H 3.74 and 4.23), as well as to the methylene fragment at δ_H 4.7 isolated from other aliphatic groups by the chain of chemical bonds. The ¹³C{¹H} NMR spectrum of complex **4** (see Fig. 2) confirms the presence of three different types of aliphatic carbon atoms in its molecule (δ_C 63.1, 64.6, and 71.3). In

* Dedicated to Academician of the Russian Academy of Sciences R. Z. Sagdeev on the occasion of his 70th birthday.

Scheme 1



addition, this spectrum exhibits signals for the carbon atoms of the phenyl substituents in the chelate ribbed fragments of the macrobicyclic ligand, their number indicating that the macrobicyclic molecule lacks the mirror plane defined by the encapsulated metal ion and the centers of the C—C bonds. This conclusion is also confirmed by the presence of the downfield signals at δ_C 154.5, 159.0, and 159.3 attributable at least to three different types of azomethine carbon atoms. Finally, the absence of the elements of symmetry in the molecule **4** is confirmed by the

^{19}F NMR spectrum of the complex in solution (see Fig. 3), which contains two partially overlapped sets of signals, each of which is formed by four lines of equal intensity. Such a pattern in the ^{19}F NMR spectra is characteristic of clathrochelates with two slightly nonequivalent cross-linking FBO_3 fragments.

All the lines in the NMR spectra were completely assigned using 2D HSQC and HMBC heteronuclear chemical shift correlations. The ^1H — ^{13}C NMR HSQC spectrum allowed us to assign signals for the carbon atoms and

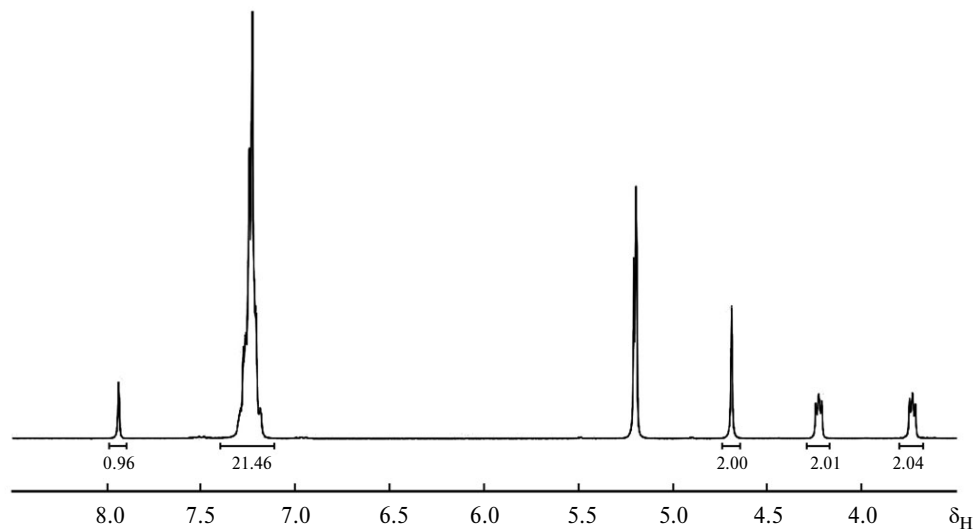


Fig. 1. The ^1H NMR spectrum of clathrochelate **4** in CD_2Cl_2 .

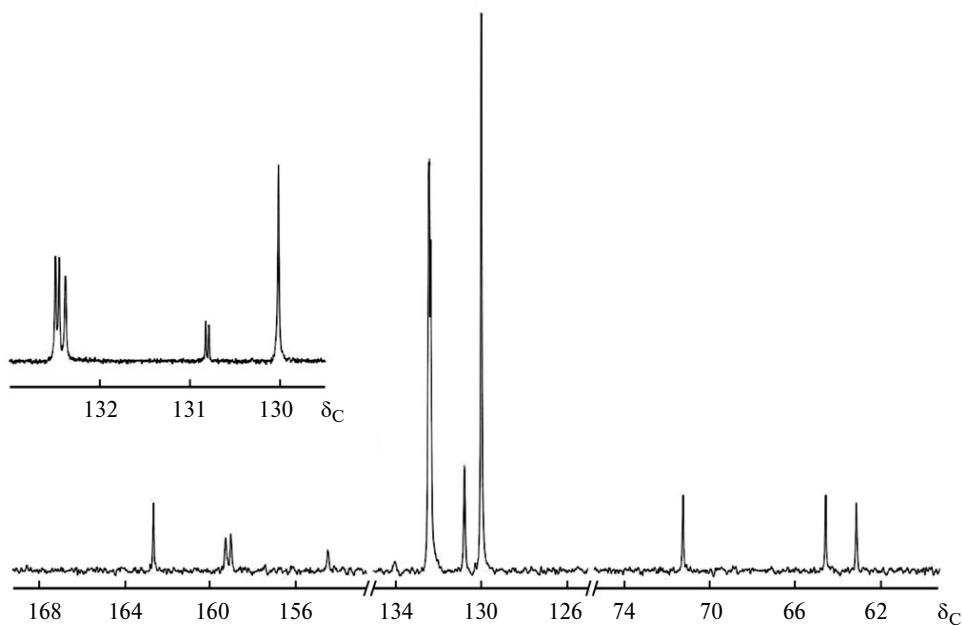


Fig. 2. The $^{13}\text{C}\{^1\text{H}\}$ NMR spectrum of complex **4** in CD_2Cl_2 .

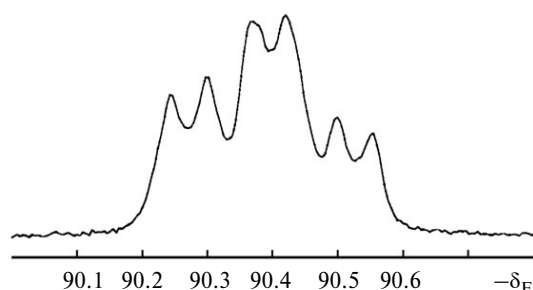


Fig. 3. The ^{19}F NMR spectrum of macrobicycle **4** in CD_2Cl_2 .

the protons directly bonded to them (Fig. 4), whereas the ^1H – ^{13}C NMR HMBC spectrum (Fig. 5) contained information on the more distant (through from two to four chemical bonds) proton–carbon interactions. In addition, in the HMBC spectrum for the signal with δ_{C} 162.7, two peaks were found at the distance of 113 Hz from the signal for the proton bound to the corresponding carbon atom ($\delta_{\text{H}} = 7.9$). Therefore, this pair of atoms is characterized by a spin-spin coupling constant $J_{\text{H}-^{13}\text{C}} = 226$ Hz, and, consequently, is an aldehyde group. The signals in the ^1H

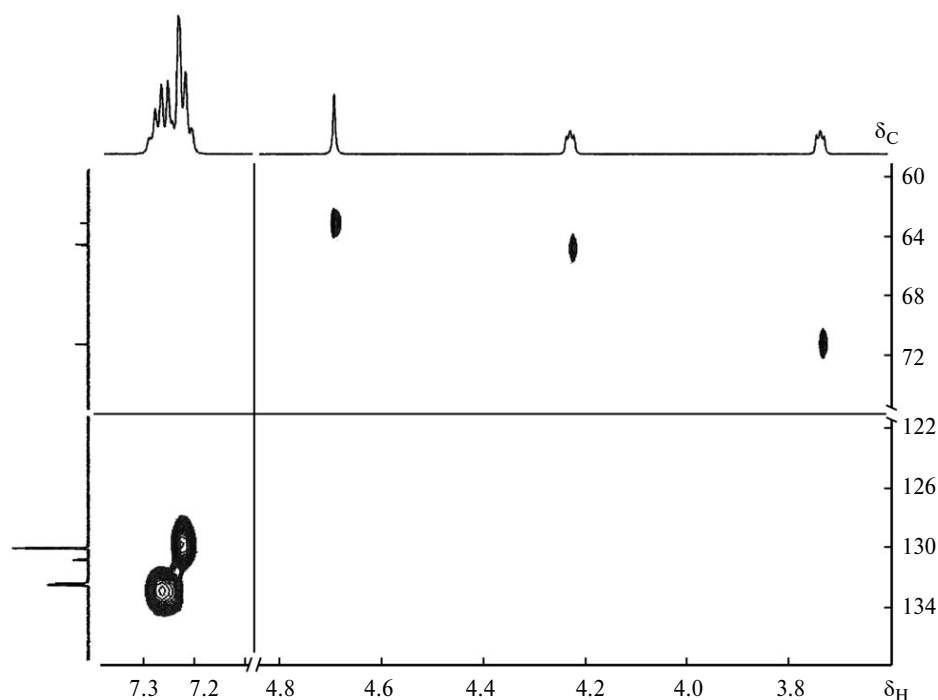


Fig. 4. The ^1H – ^{13}C HSQC NMR spectrum of complex **4**.

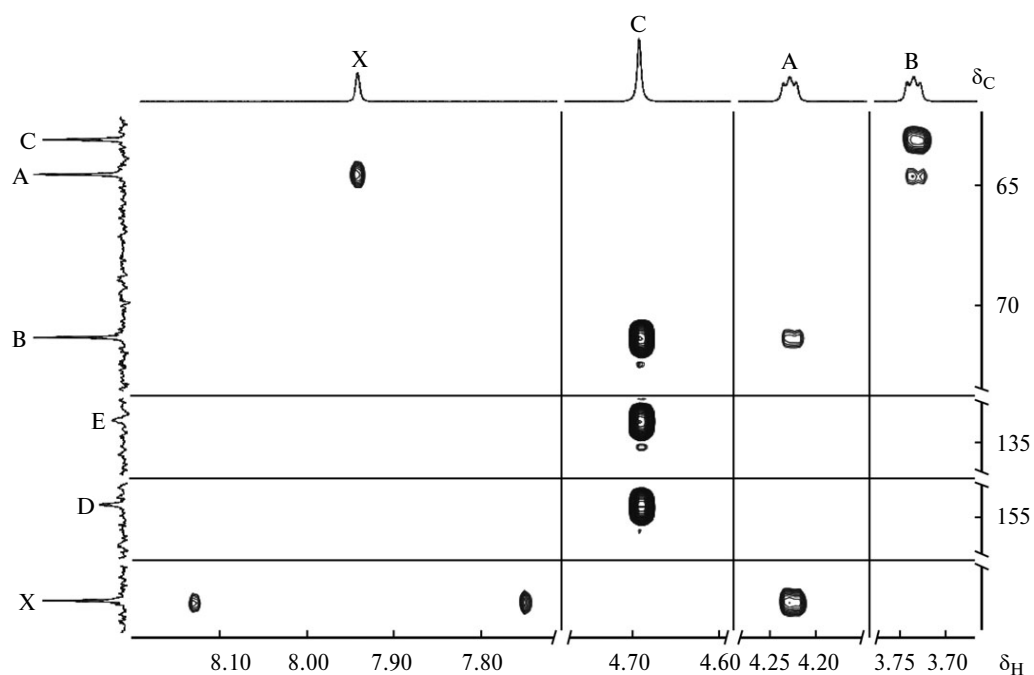


Fig. 5. The ^1H – ^{13}C HMBC NMR spectrum of clathrochelate **4**.

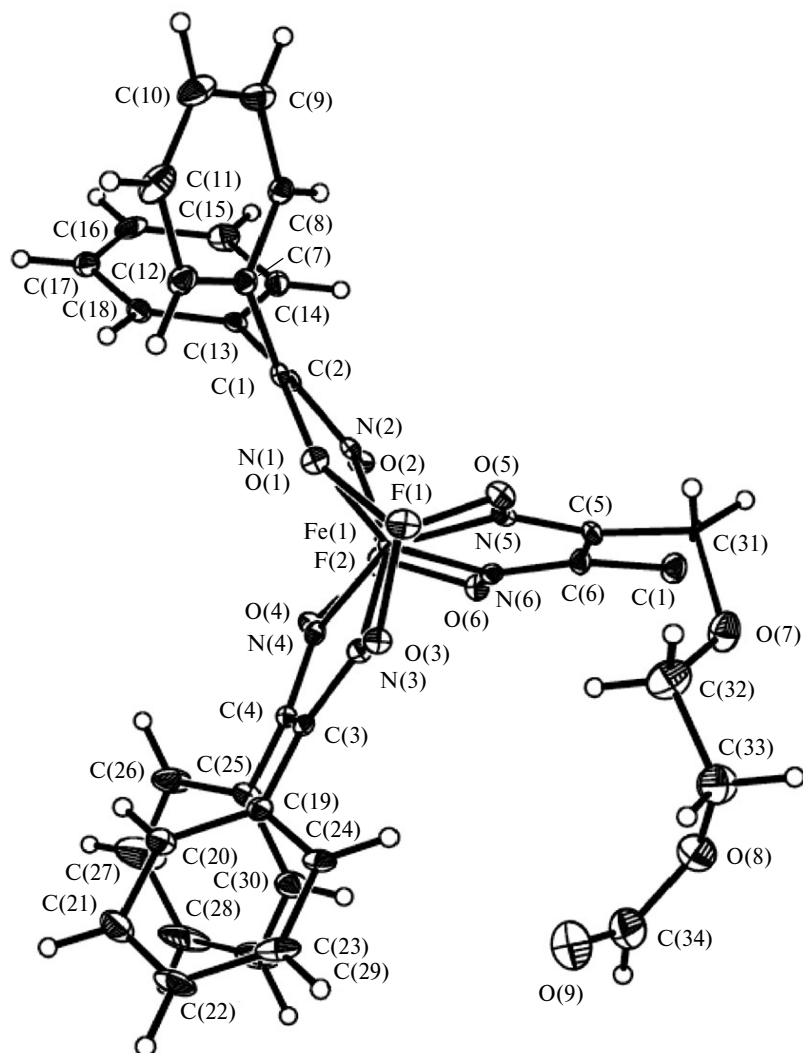


Fig. 6. The molecular structure of clathrochelate $\text{FeBd}_2(\text{ClGm}(\text{CH}_2\text{O}(\text{CH}_2)_2\text{OCHO}))(\text{BF}_4)_2$ (type A).

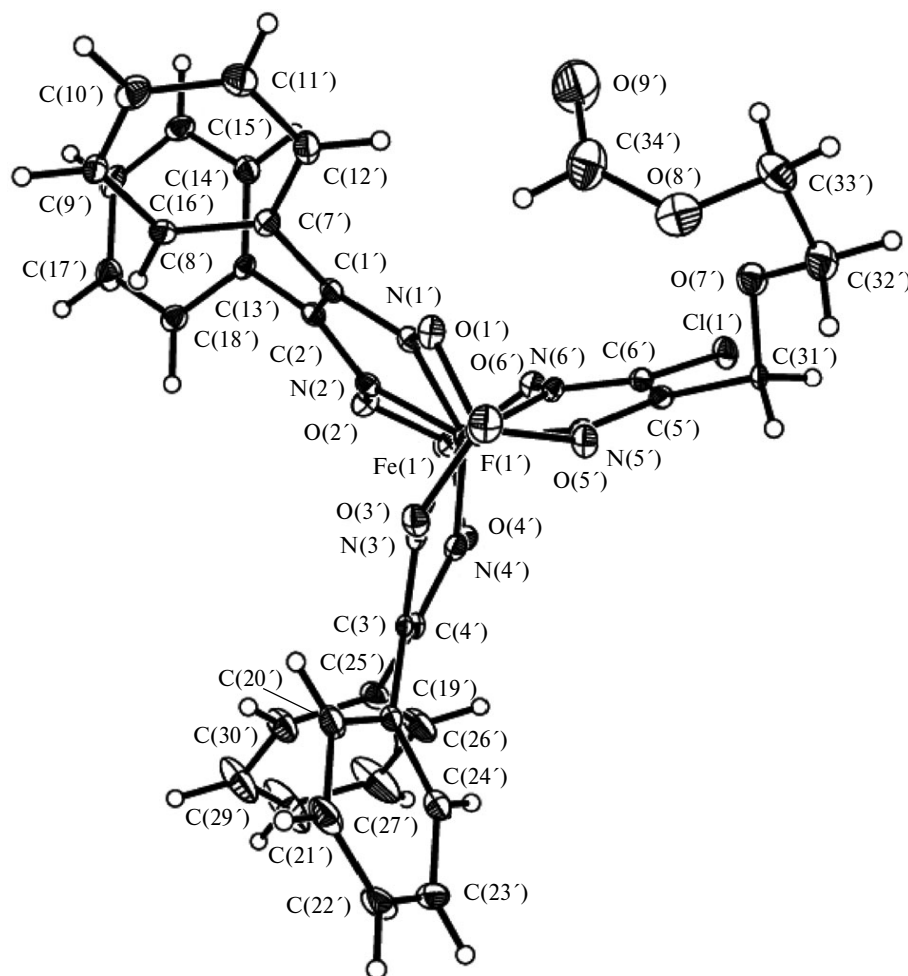


Fig. 7. The molecular structure of clathrochelate $\text{FeBd}_2(\text{ClGm}(\text{CH}_2\text{O}(\text{CH}_2)_2\text{OCHO}))(\text{BF})_2$ (type **B**).

and ^{13}C NMR spectra were finally assigned based on the analysis of the corresponding HMBC spectra.

The X-ray diffraction data show that the crystal $\text{FeBd}_2\cdot\{\text{ClGm}[\text{CH}_2\text{O}(\text{CH}_2)_2\text{OCHO}]\}(\text{BF})_2\cdot\text{C}_6\text{H}_6$ contains two independent molecules of clathrochelate $\text{FeBd}_2\{\text{ClGm}[\text{CH}_2\text{O}(\text{CH}_2)_2\text{OCHO}]\}(\text{BF})_2$ (types **A** and **B**) (Figs 6 and 7) differing in the conformation of the aldehyde-bearing ribbed substituent and by the slight turn of the phenyl substituents in one of the α -benzyldioximate chelate fragments of their macrobicyclic ligand (Fig. 8). The crystal also contains the solvent benzene molecules.

The geometry of the coordination polyhedron FeN_6 of the encapsulated iron(II) ion is the intermediate between a trigonal prism (TP, a distortion angle $\varphi = 0^\circ$) and a trigonal antiprism (TAP, $\varphi = 60^\circ$): the average φ values are 24.5° (for the type **A** molecule) and 26.2° (for the type **B** molecule); the average α values (a one half of the chelate angle $\text{N}-\text{Fe}-\text{N}$) for the molecules of these both types are the same (39.3°). As a consequence, the heights h of their TP–TAP-coordination polyhedrons are slightly different (Table. 1). The angle φ in the type **B** macrobicyclic is more

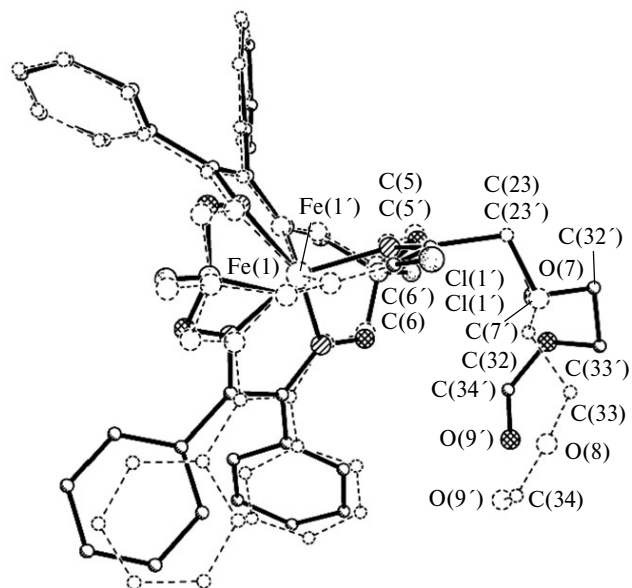


Fig. 8. The structural differences in clathrochelate molecules $\text{FeBd}_2\cdot(\text{ClGm}(\text{CH}_2\text{O}(\text{CH}_2)_2\text{OCHO}))(\text{BF})_2$ of the two types, **A** and **B**.

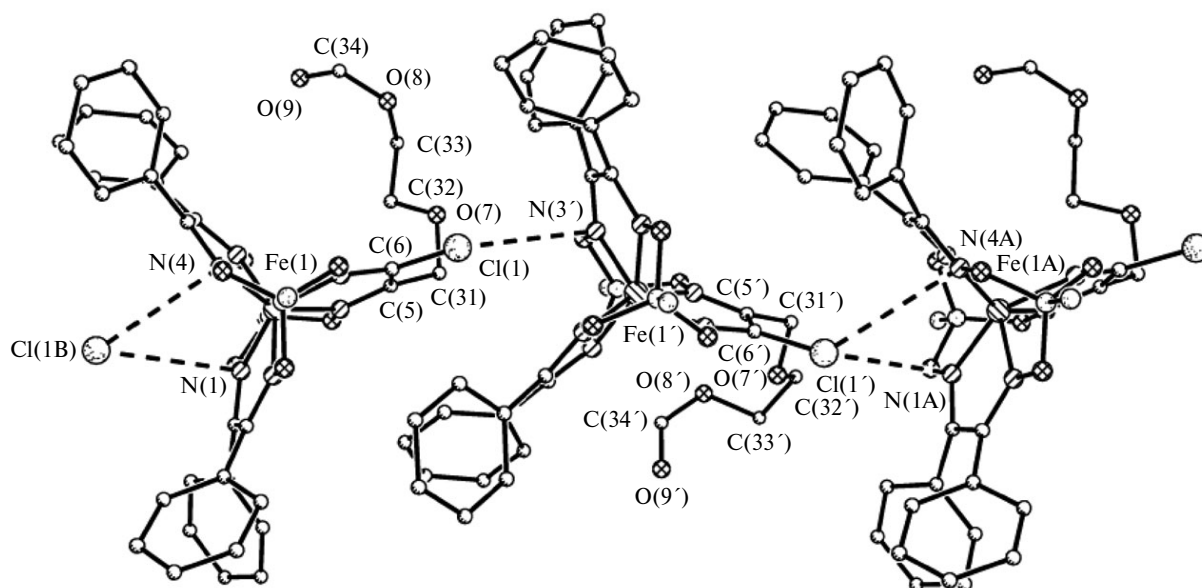


Fig. 9. Formation of chains of clathrochelate molecules in the crystal $\text{FeBd}_2(\text{ClGm}(\text{CH}_2\text{O}(\text{CH}_2)_2\text{OCHO}))(\text{BF}_3)_2 \cdot \text{C}_6\text{H}_6$ and the shortened contacts between these molecules (shown in the dashed lines).

Table 1. Some geometric parameters of the clathrochelate molecules $\text{FeBd}_2(\text{ClGm}(\text{CH}_2\text{O}(\text{CH}_2)_2\text{OCHO}))(\text{BF}_3)_2$ of the two types, **A** and **B**

Parameter	Type A	Type B
Bond $d/\text{\AA}$		
Fe(1)—N(1)	1.908(3)	1.901(3)
Fe(1)—N(3)	1.915(3)	1.908(3)
Fe(1)—N(5)	1.915(3)	1.913(3)
Fe(1)—N(2)	1.909(3)	1.913(3)
Fe(1)—N(4)	1.919(3)	1.899(3)
Fe(1)—N(6)	1.913(3)	1.903(3)
C(1)—C(2)	1.463(5)	1.444(5)
C(3)—C(4)	1.466(5)	1.465(6)
C(5)—C(6)	1.430(5)	1.441(5)
C(6)—Cl(1)	1.704(4)	1.705(4)
Bond angle ω/deg		
N(1)—Fe(1)—N(2)	78.6(1)	78.3(1)
N(3)—Fe(1)—N(4)	78.2(1)	78.3(1)
N(5)—Fe(1)—N(6)	78.7(1)	79.2(1)
Distortion angle ϕ/deg		
	24.4, 24.5, 24.6	26.5, 26.1, 25.9
Bite angle α/deg		
	39.3, 39.1, 39.4	39.2, 39.2, 39.6
Height* $h/\text{\AA}$		
	2.33	2.32

* The coordination polyhedron height.

acute (by 1.8°) than that in the type **A** clathrochelate molecule. Apparently, such a difference in the average ϕ values is due to the steric factors caused by the conformational differences of the ribbed aldehyde-bearing substituent in the type **A** and **B** molecules in the $\text{FeBd}_2(\text{ClGm}(\text{CH}_2\text{O}(\text{CH}_2)_2\text{OCHO}))(\text{BF}_3)_2 \cdot \text{C}_6\text{H}_6$ crystal.

The differences in the environment of the type **A** and **B** molecules in the crystal can also be caused by steric factors due to the different conformations of this substituent. In the crystal, these independent clathrochelate molecules form chains stretched along the crystallographic axis *b* due to the strong intermolecular contact $\text{Cl}(1)\dots\text{N}(3')$ ($3.194(3)$ Å) and weaker contacts $\text{Cl}(1)\dots\text{N}(1)$ ($3.371(3)$ Å) and $\text{Cl}(1)\dots\text{N}(4)$ ($3.426(3)$ Å) (Fig. 9). The solvent benzene molecules in the crystal $\text{FeBd}_2(\text{ClGm}(\text{CH}_2\text{O}(\text{CH}_2)_2\text{OCHO}))(\text{BF}_3)_2 \cdot \text{C}_6\text{H}_6$ occupy the cavities between these chains and do not form any shortened interatomic contacts with the macrobicyclic molecules (Fig. 10).

In conclusion, we unambiguously confirmed the fact of the oxidative cleavage of a carbon—carbon bond in 1,4-dioxane ring bound to the chelate α -dioximate fragment of the clathrochelate skeleton. The oxidative degradation of 1,4-dioxane has been observed earlier under photocatalysis conditions^{16,17} and sonochemical decomposition.¹⁸ In all these cases, ethylene glycol diformate as the product of symmetric oxidative cleavage of a carbon—carbon bond in the 1,4-dioxane ring was detected among the main oxidation products. We suggest that similar unsymmetric oxidation of the 1,4-dioxan-2-yl ribbed substituent in the α -dioximate fragment of the clathrochelate skeleton leads to the formation of clathrochelate **4**.

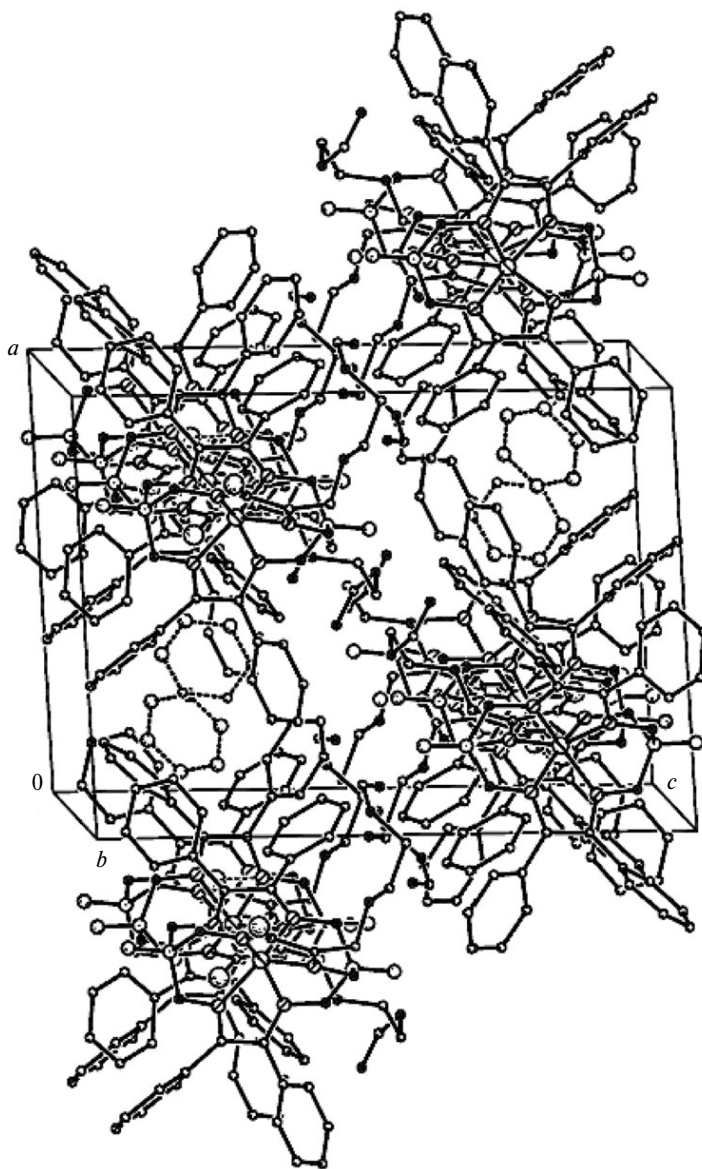


Fig. 10. The crystal structure of the complex $\text{FeBd}_2(\text{ClGm}(\text{CH}_2\text{O}(\text{CH}_2)_2\text{OCHO}))(\text{BF}_3)_2 \cdot \text{C}_6\text{H}_6$. The solvent benzene molecules (shown in the dotted lines) occupy the cavities between the chains formed by the clathrochelate molecules.

Experimental

Clathrochelate precursor **1** was obtained according to the known procedure.¹⁹ 1,4-Dioxane was purified by sequential distillation over KOH and metallic sodium. For accumulation of hydroperoxide, 1,4-dioxane was kept under light in contact with air for 2–3 weeks.

Elemental analysis for carbon, hydrogen, and nitrogen was performed on a Carlo Erba, model 1106 microanalyser.

MALDI-TOF mass spectra were recorded on an Autoflex Bruker time-of-flight MALDI-TOF-MS spectrometer in the reflecto-mol mode. The ionization was induced by the UV laser with the wavelength of 336 nm. The samples were applied to a nickel plate, 2,5-dihydroxybenzoic acid was used as a matrix. The accuracy of the measurements was 0.1%.

17-Chloro-1,8-bis(2-fluorobora)-18-(2-formyloxyethoxymethyl)-4,5,11,12-tetraphenyl-2,7,9,14,15,20-hexaoxa-3,6,10,13,16,19-hexaazabicyclo[6.6.6]eicosa-3,5,10,12,16,18-hexaene(2-iron(2+)) complex (4). The complex $\text{FeBd}_2(\text{Cl}_2\text{Gm})(\text{BF}_3)_2$ (0.105 g, 0.14 mmol) was dissolved in 1,4-dioxane (30 mL) and the solution was refluxed for 5.5 h, monitoring the reaction progress by TLC. The TLC data showed formation of monosubstituted 1,4-dioxan-2-yl clathrochelate in the reaction mixture. Then, metallic sodium (~0.3 g) was added and the reaction mixture was refluxed during several days for 3–5 h each day. After accumulation of the reaction product stopped (TLC data), the solution was filtered, and the reaction mixture was concentrated on a rotary evaporator to dryness. The solid residue was dissolved in chloroform and separated by column chromatography (1×20 cm column, silica gel Merck 9385, eluent CHCl_3), col-

lecting the fraction followed the clathrochelate precursor. This elute was concentrated in air, and the solid residue was recrystallized from a 3 : 1 dichloromethane—heptane solvent mixture. The yield was 0.345 g (30%). Found (%): C, 49.96; H, 3.48; N, 10.23. Calculated (%): $C_{34}H_{27}N_6O_9B_2F_2ClFe$. C, 50.14; H, 3.34; N, 10.32. MALDI-TOF MS, m/z (I (%)) (positive range): 701 $[M - CH_2O(CH_2)_2O(HC=O)]^+$ (20), 724 $[M + Na^+ - CH_2O(CH_2)_2O(HC=O)]^+$ (35), 740 $[M + K^+ - CH_2O(CH_2)_2O(HC=O)]^+$ (25), 755 $[M - CH_2O(HC=O)]^+$ (100), 771 $[M - CH_2 - HC=O]^+$ (30), 798 $[M - O]^+$ (80), 814 $[M]^+$ (70), 837 $[M + Na^+]^+$ (75), 853 $[M + K^+]^+$ (25); (negative range): -755 $[M - CH_2O(HC=O)]^-$ (100), -771 $[M - CH_2 - HC=O]^-$ (150), -798 $[M - O]^-$ (40), -814 $[M]^-$ (45).

X-ray diffraction studies. Single crystals of the complex $FeBd_2(ClGm(CH_2O(CH_2)_2OCHO))(BF)_2 \cdot C_6H_6$, suitable for X-ray diffraction experiment were obtained by the slow concentration of the clathrochelate **4** solution in a 1 : 1 benzene—isooctane mixture.

The red plates of the crystals $C_{34}H_{27}B_2ClF_2FeN_6O_9 \cdot C_6H_6$ ($M = 892.64$) at 100 K are triclinic, $a = 13.466(1)$ Å, $b = 15.979(1)$ Å, $c = 18.461(1)$ Å, $\alpha = 94.163(2)$, $\beta = 93.089(2)$, $\gamma = 91.130(2)^\circ$, $V = 3954.8(5)$ Å³, space group $P1^-$, $Z = 4$, $d_{calc} = 1.499$ g cm⁻³. Experimental set of 37812 reflections was obtained on a Bruker APEX II CCD diffractometer equipped with graphite monochromator (λ Mo-K α irradiation, $2\theta_{max} = 52.00^\circ$) from a single crystal $0.30 \times 0.25 \times 0.18$ mm in size. The refinement was made for 15508 independent reflections ($R_{int} = 0.0755$). Absorption ($\mu = 0.523$ mm⁻¹) was applied using the SADABS program,²⁰ the T_{max} and T_{min} transmission coefficients were equal to 0.912 and 0.859, respectively. The structure was solved by the direct method, all the nonhydrogen atoms were localized in the differential syntheses of electron density and refined on F^2_{hkl} in anisotropic approximation. All the hydrogen atoms were placed into the geometrically calculated positions and refined using the riding model with $U(H) = 1.2 U(C)$, where $U(C)$ is the equivalent temperature factor of a carbon atom bound to the corresponding hydrogen atom. The refinement convergence on all the independent reflections $wR_2 = 0.1156$, GOOF = 1.031 ($R_1 = 0.0560$ on 9559 reflections with $I > 2\sigma$), number of refined parameters, 1075.

SHELXTL PLUS 5 program package was used for all the calculations (see Ref. 21).

This work was financially supported by the Russian Foundation for Basic Research (Project Nos 09-03-00540 and 10-03-00403).

References

1. Y. Z. Voloshin, N. A. Kostromina, R. Krämer, *Clathrochelates: synthesis, structure and properties*, Elsevier, Amsterdam, 2002.
2. Y. Z. Voloshin, O. A. Varzatskii, T. E. Kron, V. K. Belsky, V. E. Zavodnik, A. V. Palchik, *Inorg. Chem.*, 2000, **39**, 1907.
3. Y. Z. Voloshin, V. E. Zavodnik, O. A. Varzatskii, V. K. Belsky, A. V. Palchik, N. G. Strizhakova, I. I. Vorontsov, M. Y. Antipin, *Dalton Trans.*, 2002, 1193.
4. Y. Z. Voloshin, O. A. Varzatskii, T. E. Kron, V. K. Belsky, V. E. Zavodnik, N. G. Strizhakova, V. A. Nadtochenko, V. A. Smirnov, *Dalton Trans.*, 2002, 1203.
5. Y. Z. Voloshin, O. A. Varzatskii, A. V. Palchik, I. I. Vorontsov, M. Y. Antipin, E. G. Lebed, *Inorg. Chim. Acta*, 2005, **358**, 131.
6. Y. Z. Voloshin, O. A. Varzatskii, A. V. Palchik, Z. A. Starikova, M. Y. Antipin, E. G. Lebed, Y. N. Bubnov, *Inorg. Chim. Acta*, 2006, **359**, 553.
7. Y. Z. Voloshin, O. A. Varzatskii, A. S. Belov, Z. A. Starikova, K. Y. Suponitsky, V. V. Novikov, Y. N. Bubnov, *Inorg. Chem.*, 2008, **47**, 2155.
8. Y. Z. Voloshin, O. A. Varzatskii, V. V. Novikov, N. G. Strizhakova, I. I. Vorontsov, A. V. Vologzhanina, K. A. Lysenko, G. V. Romanenko, M. V. Fedin, V. I. Ovcharenko, Y. N. Bubnov, *Eur. J. Inorg. Chem.*, 2010, 5401.
9. Y. Z. Voloshin, O. A. Varzatskii, A. S. Belov, Z. A. Starikova, A. V. Dolganov, V. V. Novikov, Y. N. Bubnov, *Inorg. Chim. Acta*, 2011, **370**, 322.
10. M. A. Vershinin, A. B. Burdukov, E. G. Boguslavskii, N. V. Pervukhina, N. V. Kuratieva, I. V. Eltsov, V. A. Reznikov, O. A. Varzatskii, Y. Z. Voloshin, Y. N. Bubnov, *Inorg. Chim. Acta*, 2011, **366**, 91.
11. O. A. Varzatskii, Y. Z. Voloshin, P. A. Stuzhin, S. V. Shul'ga, S. V. Volkov, A. V. Vologzhanina, E. G. Lebed, Y. N. Bubnov, *Inorg. Chem. Commun.*, 2011, **14**, 1504.
12. M. A. Vershinin, A. B. Burdukov, I. V. Eltsov, V. A. Reznikov, E. G. Boguslavsky, Y. Z. Voloshin, *Polyhedron*, 2011, **30**, 1233.
13. J. Gierer, I. Pettersson, *Acta Chem. Scand.*, 1968, **22**, 3183.
14. D. E. Kruglov, O. G. Safiev, S. S. Zlotskii, D. L. Rakhmankulov, *Khim. Geterotsikl. Soedin.*, 1983, 1192 [*Chem. Heterocycl. Compd. (Engl. Transl.)*, 1983].
15. T. Sueda, Y. Takeuchi, T. Suefuji, M. Ochiai, *Molecules*, 2005, **10**, 195.
16. M. Mehrvar, W. A. Anderson, M. Moo-Young, *Intern. J. Photoenergy*, 2000, **2**, 67.
17. V. Maurino, P. Calza, C. Minero, E. Pelizzetti, M. Vincenti, *Chemoshpere*, 1997, **35**, 2675.
18. M. A. Beckett, I. Hua, *Environ. Sci. Technol.*, 2000, **34**, 3944.
19. Y. Z. Voloshin, V. E. Zavodnik, O. A. Varzatskii, V. K. Belsky, I. I. Vorontsov, M. Y. Antipin, *Inorg. Chim. Acta*, 2001, **321**, 116.
20. Bruker, Programs APEX II, version 2.0-1; SAINT, version 7.23A; SADABS, version 2004/1; XPREP, version 2005/2.
21. G. M. Sheldrick, *Acta Crystallogr.*, 2008, **A64**, 112.

Received September 27, 2011;
in revised form November 25, 2011